Effect of radiative cooling on the relation between Cloud and sea surface temperature

Chung-Hsiung Sui[*1], Chang-Hoi Ho[2], Ming-Dah Chou[1], Ka-Ming Lau[1], and Xiaofan Li[1]

[1]NASA/Goddard Space Flight Center, Greenbelt, Maryland, USA

[2]Seoul National University, Seoul, Korea

Index:

1655 Water cycles (1836)

3359 Radiative processes

3314 Convective processes

3309 Climatology (1620)

Submitted to Geophysical Research Letters

(September 14, 2000)

[*] Corresponding author: Chung-Hsiung Sui, Goddard Space Flight Center, Mail code 913, Greenbelt, MD 20817. Telephone: 301-614-6187, Fax: 301-614-6307, E-mail: sui@climate.gsfc.nasa.gov

Abstract. We show evidence that convection over the Pacific warm pool is regulated by radiative cooling in the surrounding subsiding atmosphere over the cold pool. This is because the strength of subsidence is limited by radiative cooling which has a small variability. As a result, the area of radiatively driven subsidence expands to produce an enhanced mass exchange between the warm pool and cold pool in response to enhanced SST contrast between warm pool and surrounding cold pool (dSST). This acts against increased clouds by enhanced upward mass flux over the warm pool, and produces less cloudy (more clear) regions over the warm pool when dSST is stronger than normal.

Index:

1656 Water cycles (1836)

3360 Radiative processes

3315 Convective processes

3310 Climatology (1620)

Introduction

Water vapor and clouds play an important role in maintaining the earth climate. Water vapor is mostly recognized for a positive climate feedback process, i.e. water vapor, being transparent to incoming solar radiation but opaque to outgoing longwave radiation, produces a warmer atmosphere that can retain more moisture thus more greenhouse effect. This is supported by observations that the area-mean greenhouse trapping of the clear-sky in the tropics generally increases from cold to warm sea surface temperature (Zhang et al. 1996; Soden 1997). However, Lindzen (1990) suggested that increased convection in a warmer climate would dry the upper troposphere by detraining air at higher altitude. Consequently, he argued that the positive water vapor feedback might not hold. Lindzen's hypothesis motivated several observational analyses that generally reached the opposite conclusion, i.e. increased convection results in a moistening of the upper troposphere. But Chou (1994) found the area-mean clear-sky greenhouse effect was smaller during the warmer month of April 1987 than during the colder month of April 1985. The observed decrease in greenhouse trapping with increased surface temperature was most evident over the dry subtropical regions. Chou's analysis reveals that the change in the relative area of dry and subsiding versus moist and convective regions determines the sign of area-mean clear sky water vapor greenhouse trapping. Through consideration of tropical heat budget, Pierrehumbert (1995) emphasized that the main determinant of tropical climate is the clear-sky water vapor greenhouse effect averaged over the entire tropics. Recently, Lindzen et al. (2000) showed observational evidence that area-mean clouds over the warm pool reduces by about 15% for a 1°C increase of the cloud-weighted sea surface temperature (SST). The radiative implications of the observed cloud-SST relation are assessed in a 2-dimensional radiative-convective model that shows a negative feedback in the global climate.

In addition to the cloud/water vapor greenhouse effect, clouds also cool the climate system by reflecting solar radiation back to space. Ramanathan and Collins (1991) proposed a regulation of tropical SST by cloud albedo effect. This hypothesis causes many debates about the role of local and remote processes in determining the SST-cloud relation (see Lau et al. 1994 and references therein for details).

The above discussions indicate that local and remote processes determining the relative area of the dry and subsiding versus moist and convective regions are key climate issues. In this study, we show evidence that atmospheric radiative cooling in the subsidence region is a key process in determining the relative area of the two regions, and regulating cloud-SST relation.

Results

First, we examine the SST-cloud relation in the tropical deep convective regime and the surrounding subsidence regime in a 2-dimensional cumulus ensemble model (CEM). The CEM resolves convective-scale motion and clouds in a high-resolution non-hydrostatic dynamic system including turbulence, cloud microphysics, and radiation (Tao and Simpson 1993; Sui et al. 1994). We carry out experiments in an ocean domain of 5120 km. Experiment R, R1, and R2 are designed with an imposed warm-pool SST specified 2.5, 3.5, and 4.5^{o}C higher than the cold-pool SST that is specified at 26°C, and an imposed domain-mean vertical velocity. The area ratio of cold pool to warm pool is 2.2. The resultant time mean precipitation increases but the precipitating area decreases with increasing SST contrast between the warm pool and cold pool ($dSST \equiv SST_{w.pool} - SST_{c.pool}$). This is caused by heat balance between radiative cooling and subsidence warming in the *subsidence regime*. Because radiative cooling remains almost unchanged, the strength of subsidence is capped. To produce an enhanced mass exchange between the warm pool and surrounding cold pool in response to enhanced dSST, the area of subsidence expands.

Thus a stronger dSST produces an enhanced overturning circulation with a broader uniform sinking branch, and a narrower and stronger rising branch. The overall model response in different low-boundary forcing condition is shown schematically in Fig. 1.

The asymmetric overturning circulation is essential for understanding the cloud-SST relation. Averaged over the warm (cold) pool, the vertical velocity increases (decreases) from R to R1 when low-boundary forcing condition is weak (dSST<3.5^{o}C), and remains unchanged from R1 to R2 when low-boundary forcing condition is strong (dSST≥3.5^{o}C). This arises because the area of radiatively-driven subsidence is confined within the cold pool when dSST<3.5^{o}C, and expands over the entire cold pool and part of warm pool when SST≥3.5^{o}C. Associated with the circulation, the cloud amount over warm pool increases 4% from R to R1, but decreases 2% from R1 to R2. The former reflects both the local response to warmer SST over the warm pool and the increased strength of ascending circulation in the weak surface forcing condition (dSST<3.5^{o}C). The latter is related to the dominant effect of increased area of subsidence in the strong surface forcing condition (dSST≥3.5^{o}C).

Next, we seek supporting evidence for the above model results by analyzing high cloud amount (A_{HC}) and vertical p-velocity (ω) as a function of SST. The high cloud amount is derived from the International Satellite Cloud Climatology Project (ISCCP) (Rossow and Schiffer 1991). ISCCP D2 data are averaged to 2.5^{o}x2.5^o longitude-latitude spatial resolution and monthly time scale for the period of July 1983 - August 1994. The high cloud amount is defined to be the fractional area within each grid by clouds at levels higher than 440 hPa. The vertical p-velocity is derived from NCEP/NCAR reanalysis (Kalnay et al. 1996). The data have a horizontal resolution of 2.5^{o}x2.5^o longitude-latitude and available for 1949- present. The monthly mean SST is a blended satellite and in situ measurement based on an optimum interpolation scheme (Reynolds

and Smith 1994). The data are available on a T62 Gaussian grid (~1.87^{o}x1.87^o longitude-latitude). To be consistent with the ISCCP high cloud amount and NCEP/NCAR vertical p-velocity, SST is degraded to 2.5^{o}x2.5^o longitude-latitude by linear interpolation.

The tropical Pacific within 20°S-20°N, 130°E-110°W is chosen as our analysis domain. Within it, warm pool and cold pool are separated by an isotherm so determined that the area of warm pool is 25% of the analysis domain. The corresponding SST contrast between the warm pool and cold pool (dSST) is in the range of 2-3°C, different from the range of dSST specified in the model experiments (2.5-4.5^{o}C). The difference is mostly due to the different area ratios of warm pool to cold pool, and should not be taken seriously. There exists a strong negative relation between cold pool SST and dSST due to the El Nino-Southern Oscillation (ENSO) evolution, and a weak positive relationship between warm pool SST and dSST due to the significant contribution by seasonal cycle in addition to the ENSO evolution.

Mean A_{HC} over the warm pool and cold pool as a function of dSST is shown in Fig. 2a. Over the warm pool, A_{HC} appears to be positively correlated with dSST for the weak low-boundary forcing condition (dSST<2.6^{o}C). This correlation is associated with the increased ascending (descending) motion over the warm (cold) pool with enhanced dSST as shown by the $-\omega$ at 500 hPa level in Fig. 2b. The correlation is reversed for the strong low-boundary forcing condition (dSST>2.6^{o}C), consistent with the model results discussed above. Over the cold pool, A_{HC} and $-\omega$ are negatively correlated with dSST as is expected from the expansion of subsidence area with increasing dSST discussed above. In comparison of the above analysis with model results, we note that, unlike the model experiments, the mean vertical motion in the domain of analysis varies and is expected to influence the SST-cloud/water vapor relationship. To further clarify the results, A_{HC} and ω in Fig.2 are shown in three categories of ω at 500 hPa: $(\omega-\omega_m)<-2$ mbday^{-1}

(open circles), $|\omega-\omega_m|<2$ mbday^{-1} (crosses), and $(\omega-\omega_m)>2$ mbday^{-1} (close circles), where ω_m is the time mean ω. The circulation-stratified A_{HC} as a function of dSST shows several important features. First, A_{HC} is generally highest in category 1 and lowest in category 3. Second, A_{HC}-dSST relationship discussed above is more evident in each category. The overall observational evidence is consistent with model results.

We then examine the area mean A_{HC} over the domain (20°S-20°N, 130°E-110°W) as a function of mean SST within cloudy areas, and found a similar negative cloud-SST relationship as Lindzen et al. (2000). Furthermore, the A_{HC}-SST relation is examined in the strong low-boundary forcing condition (dSST>2.6^{o}C) and the weak low-boundary forcing condition (dSST<2.3^{o}C) categories (Fig. 3). The results show that the negative relationship is most evident in the stronger than normal dSST category. This can be explained by increased ratio of cloud-free region to cloud region associated with the asymmetric overturning circulation in response to an enhanced dSST as discussed above. In the strong dSST condition, clouds are more confined over the warm pool such that the decreased cloud areas with enhanced dSST causes a more evident negative cloud-SST relation. In the weak dSST condition, the effect of asymmetric overturning circulation on clouds may be partially offset by local SST effect as shown below.

The area mean SST-cloud relation and its regulation is further considered by examining grid values of A_{HC} as a function of SST over the tropical Pacific domain in two categories: the strong low-boundary forcing condition (dSST>2.6^{o}C) and the weak low-boundary forcing condition (dSST<2.3^{o}C) (Fig. 4). Also shown in Fig. 4 are the SST histograms in the two categories that reveal less warm SST areas (27°C<SST<29.5^{o}C) and more cold SST (SST<27°C) areas in the stronger dSST category than in the weaker dSST category. The stronger dSST category is representative of the La Nina situation. Despite the differences in SST histograms, the figure reveals

some common features in the two dSST categories: 1) cloud and SST are positively correlated over warm SSTs from 28 to 29°C, and become less and even negatively correlated for SST>29°C, 2) high SST areas (>29°C) decrease rapidly. These features are consistent with previous findings (e.g. Graham and Barnett 1987; Waliser and Graham 1993; Lau et al. 1997). However, the different features between the two categories are emphasized here. First note that mean cloud amounts are generally lower over cold SST (SST<27°C) in the stronger dSST category than in the weaker dSST category. This can be explained by a broader subsidence regime in the stronger dSST category than the weaker dSST category. Second, mean cloud amounts are generally higher over warm SST (28<SST<29°C) in the stronger dSST category than in the weaker dSST category. This is expected in a stronger rising branch circulation in the stronger dSST category than the weaker dSST category. Finally, for SST>29°C, cloud amount is smaller in the stronger dSST category than in the weaker dSST category. The smaller cloud amounts lead to more high SST areas due to enhanced solar radiation in warm clear regions as inferred from the SST histogram shown in Fig. 4.

Discussion

The observed features of SST-cloud relation discussed above generally support the model results. The response of model circulation and clouds can also explain the observed SST-cloud relations. Together the model results and observations show a regulation of SST-cloud relation by the radiative cooling in the subsidence regime.

The negative correlation between cloud amount and SST shown in Fig. 3 as found in Lindzen (2000) appears to be a fundamental relation that needs to be explained. One is attributed by Lindzen (2000) to microphysics, i.e. coalescence proceeds more rapidly with increasing air temperature (linked to SST) and results in a reduced cirrus outflow. In this reasoning, cloud changes

as a response to SST changes. An opposite interpretation of the negative SST-cloud relation shown in Fig. 4 is offered by Graham and Barnett (1987) and Ramanathan and Collins (1991) that related SST changes as a response to cloud changes. In studying the cloud-SST problem, one must consider coupled ocean-atmosphere dynamics (e.g. Sun and Liu 1996). The current analysis indicates that radiative cooling in the subsidence regime plays an important role in the coupled ocean-atmosphere system by regulating SST-cloud interaction.

References

Chou, M. D., 1994: Coolness in the tropical Pacific during an El Nino episode. *J. Climate*, **7** 1684-1692.

Graham, N., and T. P. Barnett, 1987: Sea surface temperature, surface wind divergence, and convection over tropical oceans. *Science*, **238**, 657-659.

Kalnay, E., and Coauthors, 1996: The NMC/NCAR 40 year reanalysis project. *Bull. Am. Meteorol. Soc.*, **77**, 437-471.

Lau, K.-M., C.-H. Sui, M.-D. Chou, and W.-K. Tao, 1994: An inquiry into the cirrus-cloud thermostat effect for tropical sea surface temperature. *Geophys. Res. Lett*., **21**, 1157-1160.

Lau, K.-M., H-T. Wu, S. bony, 1997: The role of large-scale atmospheric circulation in the relationship between tropical convection and sea surface temperature. *J. Climate*, **10**, 381-392.

Lindzen, R. S., 1990: Some coolness concerning global warming. *Bull. Amer. Meteor. Soc*., **71**, 288-299.

Lindzen, R. S., M.-D. Chou, A. Hou, 2000: Does the earth have an adaptive infrared iris? Submitted to *Bull. Am. Meteorol. Soc*.

Pierrehumbert, R. T., 1995: Thermstats, radiator fins, and the runaway greenhouse. *J. Atmos. Sci*., **52**, 1784-1806.

Ramanathan, V., and W. Collins, 1991: Thermodynamic regulation of ocean warming by cirrus clouds deduced from observations of the 1987 El Nino. Nature, 351(B), 27-32.

Reynolds, R. W., and T. S. Smith, 1994: Improved global sea surface temperature analysis. *J. Climate*, **7**, 929-948.

Rossow, W. B., and R. A. Schiffer, 1991: ISCCP Cloud Data Products. *Bull. Am. Meteorol. Soc.*, **72**, 2-20.

Soden, B. J., 1997: Variations in the tropical greenhouse effect during El Nino. *J. Climate*. **10**, 1050-1055.

Sui, C.-H., K.-M. Lau, W.-K. Tao and J. Simpson, 1994: The tropical water and energy cycles in a cumulus ensemble model. Part 1: Equilibrium climate. *J. Atmos. Sci.*, **51**, 711-728.

Sun, D., and Liu, Z, 1996: Dynamic ocean-atmosphere coupling: A thermostat for the tropics. Science, 272, 1148-1150.

Tao, W.-K., and J. Simpson, 1993: The Goddard Cumulus Ensemble Model. Part 1: Model description. *Terrestrial, Atmospheric and Oceanic Science*, **4**, 35-72.

Waliser, E. E., and N. E. Graham, 1993, Convective cloud systems and warm-pool SSTs: Coupled interactions and self-regulation. J. Geophys. Res, 98(D7), 12881-12893.

Zhang, M. H., R. D. Cess, and S. C. Xie, 1996: Relationship between cloud radiative forcing and sea surface temperatures over the entire tropical oceans. *J. Climate*. **9**, 1374-1384.

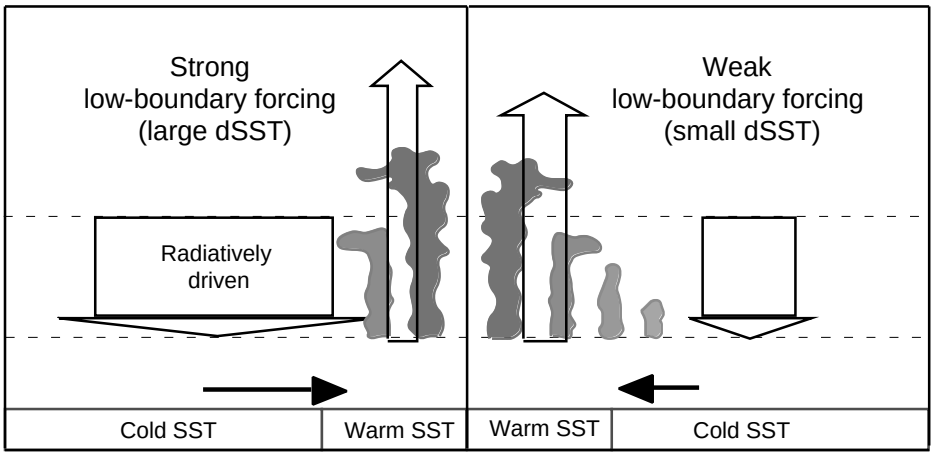

*Fig. 1 Schematic summary of tropical circulation and clouds (**V** and w by horizontal and vertical arrows) in strong & weak low-boundary forcing regimes. The area of upward and downward motion is proportional to the width of the vertical arrows, the strength of **V** and w is proportional to the length of the arrows.*

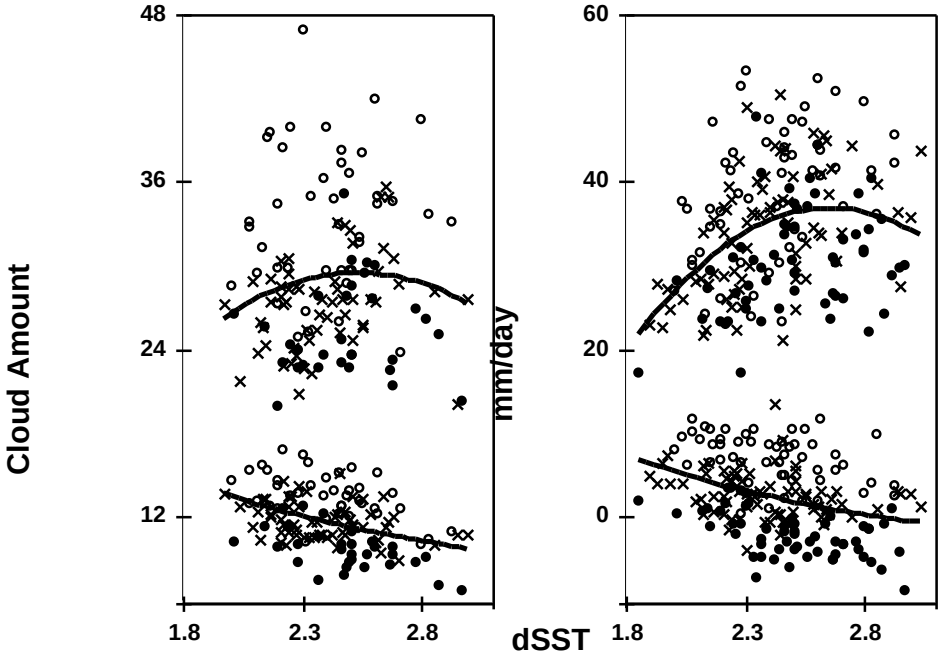

Fig.2 Scatter plot of A_{HC} (A), and -ω(500 hPa)(B) over the warm pool (upper) and cold pool (lower) as a function of dSST. o, x, and • correspond to the three categories of ω.

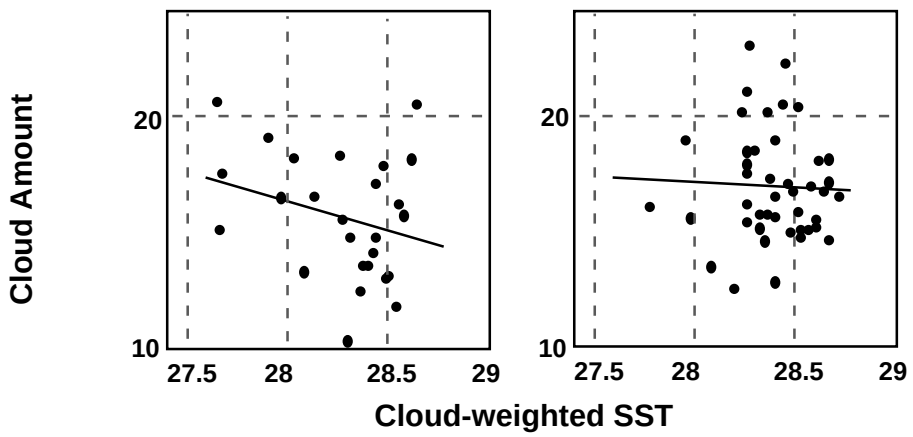

Fig. 3 Scatter plot between area mean SST and cloud weighted A_{HC} in the tropical Pacific (20°S-20°N, 130°E-110°W) for (A) dSST>2.6°C, and (B) dSST<2.3°C.

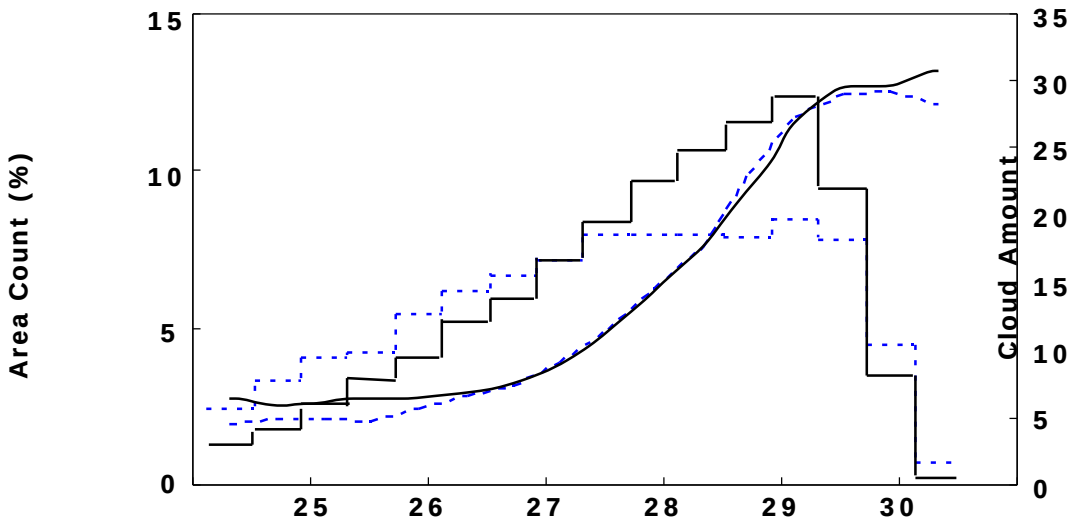

Fig. 4 Relationship between collocated A_{HC} and SST in the tropical Pacific (20°S-20°N, 130°E-110°W) for dSST>2.6°C (dashed curve), and dSST<2.3°C (solid curve), expressed as the mean A_{HC} values within every 0.4°C SST bin. The corresponding histograms of SST are also shown in terms of fractional area.